

FUNDAMENTAL NOISE STUDIES OF QUARTZ CRYSTAL RESONATORS

J.J. Gagnepain

Ecole Nationale Supérieure de Chronométrie et Micromécanique*
Besançon, France

Summary

The studies of quartz crystal oscillator frequency instabilities show they are not entirely due to electronics noise but the quartz resonator itself must be considered as a noise source. The previous investigations of resonator frequency noises (given by F. Walls) gave an important indication about their levels. This work presents the results of measurements of frequency fluctuations of quartz resonators used as passive four-ports. The noise is characterized in the frequency domain.

Several noise sources contribute to the frequency fluctuations. Correlation with external perturbations as vibrations and temperature fluctuations are studied. In the power density spectra the noise at the lowest Fourier frequencies is related with thermal effects and mainly with thermal stresses. The flicker noise level is partially related with the resonator design. Different kinds of resonators at different frequencies are used with particular plating types and shapes.

Introduction

To improve the quartz crystal oscillator stability it is important to be able to separate in the noise the part due to the resonator from the part due to the electronics. Measurements of resonator resonance frequency noise have been performed by F. Walls [1] at 5 MHz and 10 MHz. The present work is a continuation of these previous measurements.

The short-term stability is mostly limited by the additive thermal noise and therefore could be improved by increasing the driving voltage. But relatively high powers cannot be achieved because they increase the flicker noise level, and the amplitude to frequency noise conversion. On the other hand this can have an influence on the long-term stability, as the power drifts will be converted to frequency drifts.

The long-term stability is affected by the electronic components and, principally, by a change of resonator parameters with age. These phenomena are related to the technology and some mechanisms like impurity migrations inside the crystal lattice, surface transformations, and leaks in the enclosure. There is also stress relaxation in the electrodes [2]. One interesting solution is the actual development of electrodeless resonators [3].

The stability in the region from about 1 s to 100 s is limited by the flicker noise and the random walk frequency noise. These noises are direct modifications of the resonator resonance frequency. Their physical mechanisms are not understood yet and the best way to study them appears to be the use of resonators as passive devices.

Measurement System

The measurement system which has been used is similar to the one presented by F. Walls [1] but features some modifications. This system is schematically shown in Fig. 1.

Two resonators Q_1 and Q_2 , identical or made iden-

*This work is being performed at the Frequency & Time Standards Section, National Bureau of Standards, Boulder, Colorado 80302.

tical by means of the resistors r_1 , r_2 and of tuning capacitors Γ_1 and Γ_2 , are driven in transmission by the source S and their phases are compared with the double balanced mixer M_1 . An adjustable phase shifter permits one to operate the mixer at the quadrature point. The phase noise at the mixer output is proportional to the resonator's frequency fluctuations. Using the integrator I_1 and the varactor diode D_1 it is possible to lock the frequencies of both resonators together with an appropriate attack time. The second device using the mixer M_2 is used to calibrate the sensitivities (in fact to control the factor Q/w , where Q is the quality factor and w the resonance frequency) for each resonator. This is very important when any parameter in the measurement system is changed. It is also useful to lock the quartz Q_2 with the source using the integrator I_2 and the varactor diode D_2 . Special care must be taken in the adjustment of the frequency tuning and Q factors balancing in order to remove the influence of both frequency and amplitude noises from the source. The equivalent circuit is shown in Fig. 2.

Let's introduce the angular resonance frequencies ω_1 and ω_2

$$(1) \quad \omega_1^2 = 1/L_1 C_1, \quad \omega_2^2 = 1/L_2 C_2$$

the Q factors Q_1 and Q_2

$$(2) \quad Q_1 = L_1 \omega_1 / R_1, \quad Q_2 = L_2 \omega_2 / R_2$$

The capacitors Γ_1 and Γ_2 will tune the angular frequencies to the values ω'_1 and ω'_2 .

$$(3) \quad \omega'_1{}^2 = \omega_1^2 \left(1 + \frac{C_1}{\Gamma_1 + C_0}\right), \quad \omega'_2{}^2 = \omega_2^2 \left(1 + \frac{C_2}{\Gamma_2 + \gamma_0}\right).$$

The resonator tuning will force $\omega'_1 = \omega'_2$. Let's introduce the driving signal angular frequency $\omega = \omega_1 + \Delta\omega$ where $\Delta\omega$ is the difference between ω and the resonator resonance angular frequency ω_1 . After several approximations (high Q factors, $\Delta\omega$ small and $Q_1/\omega_1 \approx Q_2/\omega_2$) the phase difference ϕ at the mixer output is given by the relation:

$$(4) \quad \phi \approx 2 \Delta\omega \left(\frac{Q_1}{\omega_1} - \frac{Q_2}{\omega_2} \right) + 4 \Delta\omega^2 Q_1 \left(\frac{1}{k_1 \omega_1^2} - \frac{1}{k_2 \omega_2^2} \right) + \frac{\omega_1^2}{Q_1} \left(\frac{1}{k_2 \omega_2^2} - \frac{1}{k_1 \omega_1^2} \right)$$

with

$$(5) \quad k_1 = \frac{C_1 \Gamma_1}{C_0 (C_0 + \Gamma_1)} \quad \text{and} \quad k_2 = \frac{C_2 \Gamma_2}{\gamma_0 (\gamma_0 + \Gamma_2)}$$

The first term in the relation (4) can be cancelled out, balancing the Q/ω factors. The third term is frequency independent and can be removed, adjusting the DC output amplitude offset. In the case of $C_0 = \gamma_0$ and $C_0, \gamma_0 \leq \Gamma_1, \Gamma_2$ the relation becomes:

$$(6) \quad \phi = 2 \Delta\omega \left(\frac{Q_1}{\omega_1} - \frac{Q_2}{\omega_2} \right) + 4 Q_1 C_0 \Delta\omega^2 (L_2 - L_1) + \frac{\omega_1^2 C_0}{Q} (L_2 - L_1).$$

The source frequency fluctuations influence will be minimum for the particular value $\Delta\omega_0$ of $\Delta\omega$:

$$(7) \quad \Delta\omega_0 = - \frac{(Q_1/\omega_1 - Q_2/\omega_2)}{4 Q_1 C_0 (L_2 - L_1)}.$$

If the source frequency adjustment is achieved with a small error ϵ_0 and if the source fractional frequency fluctuations y_s are introduced, the phase noise $\delta\phi_s$ due to these source fluctuations is given by the relation:

$$(8) \quad \delta\phi_s = 8 Q_1 C_0 (L_2 - L_1) \epsilon_0 \omega_1 y_s.$$

Introducing the fractional frequency fluctuations of the resonator, y_q , we find for the corresponding phase noise $\delta\phi_q$ for the pair:

$$(9) \quad \delta\phi_q = -2\sqrt{2} Q_1 y_q.$$

For 5 MHz, 5th overtone, resonators with, for instance, $C_0 = 10 \times 10^{-12}$ F, $L_2 - L_1 = 2$ H, $\epsilon_0 = 5$ rad/s we will obtain the following ratio between both noises

$$(10) \quad \frac{\delta\phi_q}{\delta\phi_s} = 2 \times 10^3 \frac{y_q}{y_s}$$

which shows that the source noise influence can be removed with the appropriate adjustment. The curves shown in Fig. 3 represent the mixer output voltage as a function of the source frequency and the Q factor balancing. A residual noise is unbalanced because of time delay differences in the cables and circuitry. It is included in the measurement system noise and it is measured substituting resistors in place of the resonators.

The previous calculation is valid for frequencies within the resonator linewidth. For frequencies outside the linewidth it is necessary to take into account the resonator's filtering effect. If $S_y(f)$ is the power spectrum of fractional frequency fluctuations and $S_\phi(f)$, the corresponding phase spectrum, they are related by the following relation where f is the Fourier frequency:

$$(11) \quad S_\phi(f) = S_y(f) \frac{\omega_1^2}{(2\pi f)^2 + \frac{\omega_1^2}{4Q_1^2}}.$$

Moreover, the source amplitude noise is transformed into frequency noise by the resonator amplitude-frequency effect. This depends on the driving level, but there is compensation between the two resonators if they are identical. With the source* used in these studies, and a power of 1 μ W, the equivalent $S_y(f)$ (in 1 Hz bandwidth) at 1 Hz from the carrier, due to this effect is equal to 10^{-28} for regular 5 MHz, 5th overtone, resonators. The second effect of amplitude modulation will be to introduce noise at the mixer output because of the nonlinearities of the mixer. With voltage amplitude

*The source was a high quality frequency synthesizer

of 1V p.t.p. the corresponding noise is of the order of 1 nV (at 2 Hz). It is lower than the measurement system noise and, in fact it is always possible to adjust the driving levels on both the mixer inputs to minimize this noise.

Most important is the load impedance, particularly the reactive part, because any variation in this will change the resonator frequency following the relation:

$$(12) \quad \left| \frac{d\omega'_1}{\omega'_1} \right| = \frac{C_1}{2\Gamma_1} \frac{d\Gamma_1}{\Gamma_1}$$

where Γ_1 includes the tuning capacitor and the first stage amplifier input capacitor (with the assumption $\Gamma_1 > C_0$). For a 5 MHz, 5th overtone, resonator $C_1 = 4 \times 10^{-4}$ pF and, for example, with $\Gamma_1 = 100$ pF we obtain $d\omega'_1/\omega'_1 = 2 \times 10^{-6} d\Gamma_1/\Gamma_1$. It is therefore necessary to choose tuning capacitors with quality such as $d\Gamma_1/\Gamma_1 \leq 10^{-8}$.

In fact, in most oscillators the medium term stability can be limited by the fluctuations of the reactive part of the impedance, if enough care is not taken. The choice of the vibration mode of the resonator is important too, because the value of the motional capacitor C_1 is approximately inversely proportional to n^3 , where n is the overtone rank. The electrodes' size also defines the C_1 value. Therefore the higher the overtone rank and the smaller the electrode surface, the lower will be C_1 .

The noise obtained at the measurement system output is applied to a spectrum analyzer with a 1 Hz bandwidth and a 2 - 1000 Hz frequency range. At the same time this noise is filtered using a constant Q filter, in the range 0.01 - 10 Hz. The filtered voltage is converted into frequency and its mean square value measured and calculated with a computing counter. These two parts of this frequency domain phase noise measurement system thus have overlapping ranges and allow the direct measurement of $S_\phi(f)$ over a total range of $f = 0.01$ Hz to $f = 1000$ Hz.

Experimental Results

The fractional frequency fluctuation's density power spectrum $S_y(f)$ is calculated from the relation (11) where $S_\phi(f)$ is obtained as described above, taking into account the mixer sensitivity (3.7 mV/degree) and the amplifier gain (10^4).

Frequency and Plating Influence

Fig. 4 depicts the spectra of resonators at 1 MHz, 5 MHz, 10 MHz and 25 MHz. The lowest noise level is obtained with the 5 MHz crystals. In the spectra the slope of f^{-1} corresponds to flicker noise. The dotted part is the directly measured result, corrected using relation (11). At low Fourier frequencies, the spectra present slopes of f^{-2} (random walk of frequency) and f^{-3} . With the 10 MHz resonators, important differences in the flicker noise levels have been found between resonators of the same type. A resonator with a flicker noise of 4×10^{-19} (at $f = 1$ Hz) at room temperature, heated up to 90° C presented a decrease of its noise level to 1×10^{-22} , which remained unchanged after coming back to room temperature. This phenomenon may be related to stress relaxation in the electrodes [2].

Several 5 MHz resonators vibrating in the fundamental mode have been studied with circular platings and Z shaped platings, but with the same mounting. The noise

level is decreasing with the electrodes surface, but without significant proportionality. The same study performed with 5 MHz, 5th overtone, resonators using circular and rectangular platings of different surface area presents also a noise increasing with the plating area. Among this series of resonators made with the same technology, the lowest noise levels obtained at $f = 1$ Hz, using a power of $10 \mu\text{W}$ during these measurements are shown in Table I.

resonator type	sample size	$S_y(1 \text{ Hz})$
5 MHz fund. circular plating	2	5×10^{-22}
5 MHz fund. Z plating	4	1×10^{-22}
5 MHz 5th overtone circular plating	6	1×10^{-24}
5 MHz 5th overtone rectangular plating	2	1.5×10^{-23}
5 MHz 5th overtone electrodeless	2	2×10^{-25}

TABLE I.

Vibrations

The external vibrations can be "naturally" present in the room, or experimentally applied accelerations. These acceleration experiments were carried out using a loudspeaker and a power amplifier. The accelerations were measured by an piezoelectric ceramic-type accelerometer mounted close to the tested resonator.

With one 5 MHz fundamental mode resonator, a direct influence of the vibrations have been found, shown in Fig. 5a. The spectrum presents a floor and a peak in the range 8 - 20 Hz, directly related with the vibration spectrum (Fig. 5b). In fact this sensitivity was entirely due to induced vibrations of the mounting and resonator output leads and it can be easily removed using stronger leads and fixation. Similar experiments with other resonators of Table I show no direct correlation between noise spectrum and low level external vibrations.

Temperature

More significant are the temperature effects. Noise measurements have been done at different temperatures. If there was a direct correlation between the resonator temperature coefficient and the noise level, this last one should be minimum at the temperature turn-over point. Experimentally this was found not to be the case (except for very high temperature sensitivity). Under thermal perturbation the quadratic thermal properties of the crystal are not valid anymore and it becomes necessary to take into account the thermal gradients. Applying very fast temperature variations with a laser beam (power 1 mW) at different points on the crystal surface, thermal gradients and therefore thermal stresses were induced. The resulting frequency variations were measured with the previously discussed phase bridge. The frequency response of the 10 MHz resonators is shown in Fig. 6. The most sensitive points are those close to the fixation points. It is possible to calculate from these curves an equivalent temperature coefficient to compare it with the regular quadratic one. For instance, *Prototype resonators made by R. Besson, ENSCM, Besancon, France.

for the 10 MHz resonator, at room temperature the quasistatic temperature coefficient is $5.4 \text{ Hz}/^\circ\text{C}$. For the curves of Fig. 6 with a slope (df/dt) at the origin, with m the crystal mass, C its specific heat, and P the beam power, the apparent temperature coefficient a is given by the relation:

$$(13) \quad a = \left(\frac{df}{dt} \right) \frac{mC}{P}.$$

a is found equal to $50 \text{ Hz}/^\circ\text{C}$ for the worst case. The frequency variation due to thermal stresses is ten times greater than the variation due to thermal expansion and elastic coefficient changes.

For resonators with very high temperature coefficients an important noise level increase can be observed. Fig. 7 shows the noise spectrum of a double rotated cut resonator which is used as temperature sensor. Its temperature coefficient is equal to $360 \text{ Hz}/^\circ\text{C}$. If, at 1 Hz, the frequency fluctuations are totally due to thermal fluctuations, this corresponds to temperature fluctuations of $8 \mu^\circ\text{C}$.

The correlation between 10 MHz resonators frequency noise and the temperature fluctuations inside the oven has been studied using the previous temperature sensor, the frequency noise of which was measured using also a phase bridge. The resolution of this phase bridge corresponds in this case to a temperature resolution, at 1 Hz, equal to $0.2 \mu^\circ\text{C}$. Both noise voltages $e_1(\tau)$ from the 10 MHz resonators and $e_2(\tau)$ from the sensor are filtered at a given common frequency, thus converted into frequencies using voltage to frequency converters. The cross correlations function $Re_1e_2(\tau)$ and the auto-correlation functions $Re_1e_1(\tau)$ and $Re_2e_2(\tau)$ are calculated with the computing counter. The cross-correlation coefficient $K(\tau)$ is defined by the relation:

$$(14) \quad K(\tau) = \frac{Re_1e_2(\tau)}{\sqrt{Re_1e_1(0) \cdot Re_2e_2(0)}}.$$

Its maxima, at different Fourier frequencies, are shown in Table II.

Frequency	0.01 Hz	0.1 Hz	1 Hz
$K_{\max}(\tau)$	60%	30%	6%

Table II.

There is a direct correlation for low frequencies corresponding in the spectra to the frequency random walk noise. This correlation decreases quickly at frequencies where the flicker noise becomes predominant. The measurements have been done using resonators in the differential method of Fig. 1. In fact, there must be some compensation between the temperature fluctuations of the two resonators, reducing the measured correlation. At this time, a quantitative assessment of this effect appears difficult. For an individual resonator the correlation will be stronger. The correlation depends also on the sensor position with respect to the resonators and certainly the best way would be to combine resonator and sensor in the same enclosure.

Remarks

The driving power level has an influence on the flicker noise level. This has been already observed in hard driven oscillators. But these is no precise

law as has been found for excess noise in resistors [4], where the noise power density is directly proportional to the dissipated power. In quartz crystal resonators this is true for high excitation powers ($\geq 10 \mu\text{W}$), but for lower values it depends more on the crystal type and the technology used. A floor can be observed or even a noise increase. It is difficult to give interpretations of these phenomena, but they could be explained by surface effects due to impurities and vibrationally dead zones on the crystal.

The noise level is also a function of life time especially if the resonator is oscillating for the first time. Fig. 8a shows the noise level variation (at 1 Hz) versus time for 5 MHz, 5th overtone, resonators. Any perturbation of the oscillation gives also a temporary noise increase, but with different time constant, which could mean that both of these phenomena do not have the same physical origin. In Fig. 8b is shown the noise level evolution versus the time after the driving voltage has been turned off for one minute.

The thermal noise in quartz crystal resonators has never been measured. A theoretical evaluation of its value can be performed knowing the losses inside the crystal. The simplest way is to consider it as an additive noise, inducing phase fluctuations. An equivalent resonator frequency noise, giving the same phase noise, can be calculated and its power spectrum is given by the relation:

$$(15) \quad S_y(f)_{\text{thermal}} = \frac{kT}{2Q^2P}$$

where k is the Boltzmann constant, T the absolute temperature, P the dissipated power, Q the Q factor and ω_0 the resonance angular frequency. For a power of $1 \mu\text{W}$, a Q factor of 2×10^6 and at 300K $S_y(f)$ is equal to 1×10^{-27} (inside the resonator line width) and it is much lower than the measured noises.

Conclusion

Several noise sources contributing to quartz crystal resonator frequency fluctuations have been found. Among them, two main noises are to be distinguished: one related to temperature fluctuations at low Fourier frequencies, the other one causing flicker noise spectral behavior. This flicker noise could be related to several relaxation phenomena inside the crystal lattice but with some influence of environmental and surface effects which can be sometimes important.

It follows that it may be impossible to achieve in a single oscillator state-of-the-art short- and long-term stabilities at the same time. The solution could be the use of two resonators, as active and/or passive devices, driven respectively with high and low power to realize the possible stability over all Fourier frequencies. One other application is the possibility of using a passive resonator in a discriminator mode for the measurement of frequency instabilities of not so stable oscillators (or synthesizers).

From all available published material it appears that stabilities like aging of 10^{-12} per day and flicker floors in the high range of 10^{-14} could be achieved with quartz crystal devices in the near future.

Acknowledgements

This work has been carried out in the Frequency and Time Standards Section of the National Bureau of Standards. The author wishes to thank H. Hellwig for giving the opportunity to perform this study and for helpful discussions. He is deeply grateful too to F. Walls for his help and suggestions, and to R. Besson for providing the electrodeless resonators.

References

- [1] F.L. Walls, A.E. Wainwright, "Measurement of the Short-Term Stability of Quartz Crystal Resonators and the Implications for Crystal Oscillator Design and Applications," IEEE Trans. on Instrumentation and Measurement, Vol. IM-24. no. 1, March 1975.
- [2] E.P. Eer Nisse, "Quartz Resonator Frequency Shifts Arising from Electrode Stress," Proc. 29th SFC, Ft. Monmouth, NJ, 1975.
- [3] R. Besson, A New Piezoelectric Resonator Design," Proc. 30th SFC, Ft. Monmouth, NJ, 1976.
- [4] C.S. Bull, S.M. Bozic, "Excess Noise in Semi-Conducting Devices due to Fluctuations in their Characteristics when Signals are Applied," Brit. J. of Appl. Phys, Vol. 18, 1967.

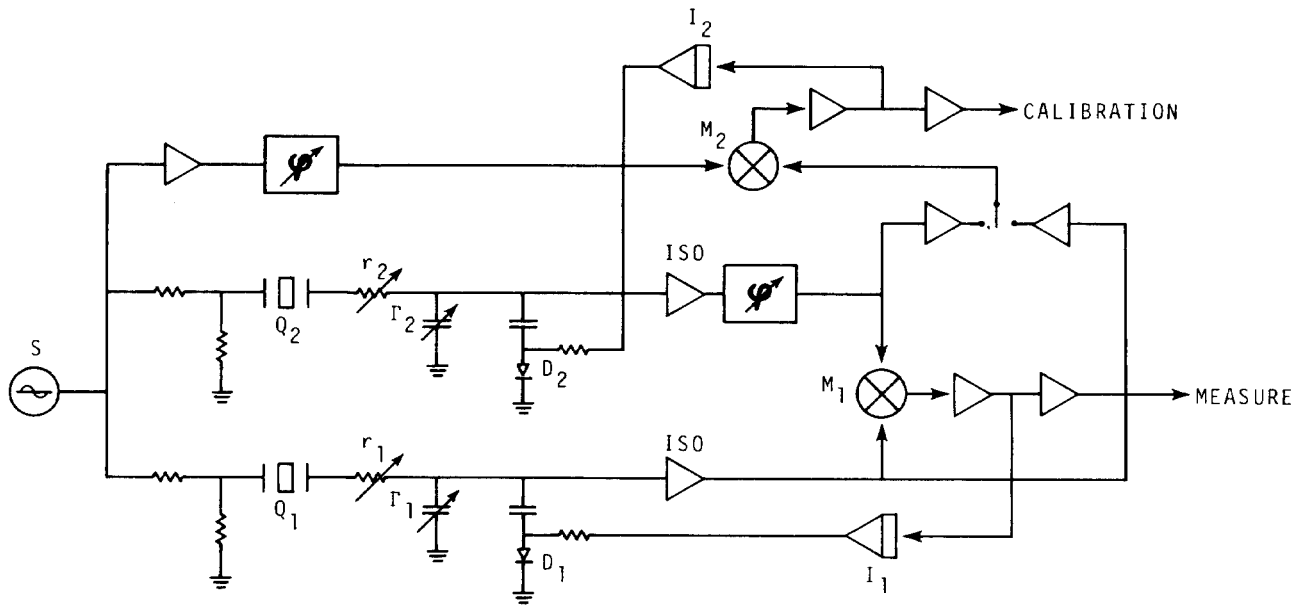


Fig. 1 Measurement system

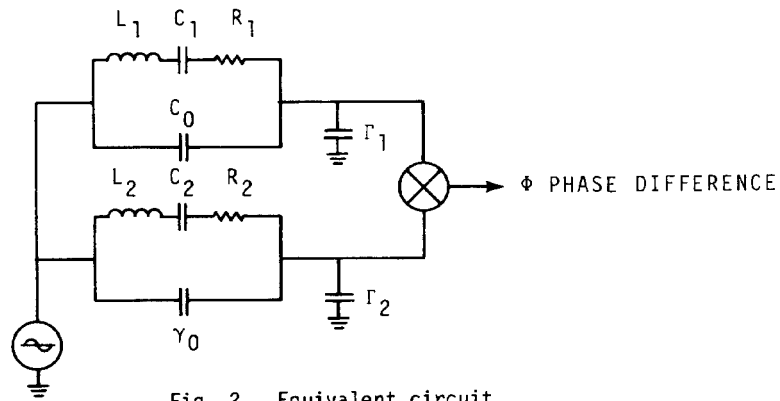


Fig. 2 Equivalent circuit

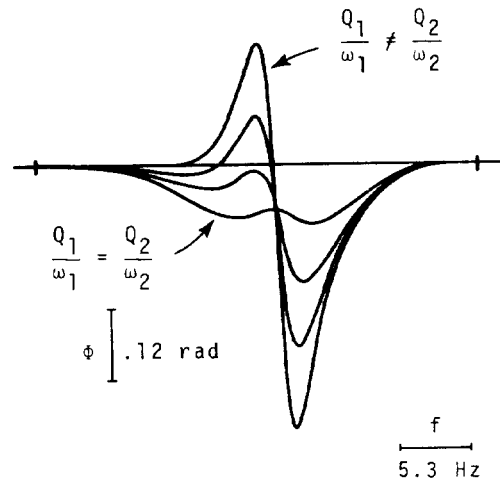


Fig. 3 Phase response of the measurement system as a function of the Q/ω factor balancing

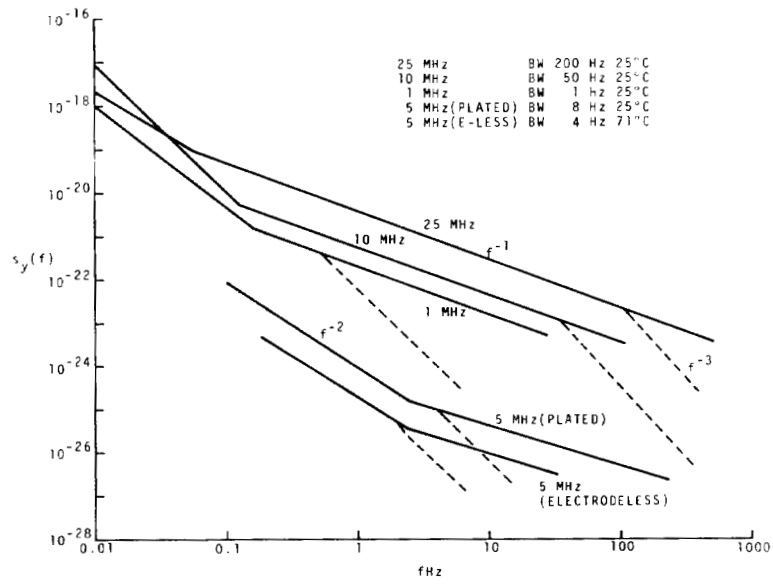


Fig. 4 Fractional frequency fluctuation's density power spectra of quartz crystal resonators at different frequencies

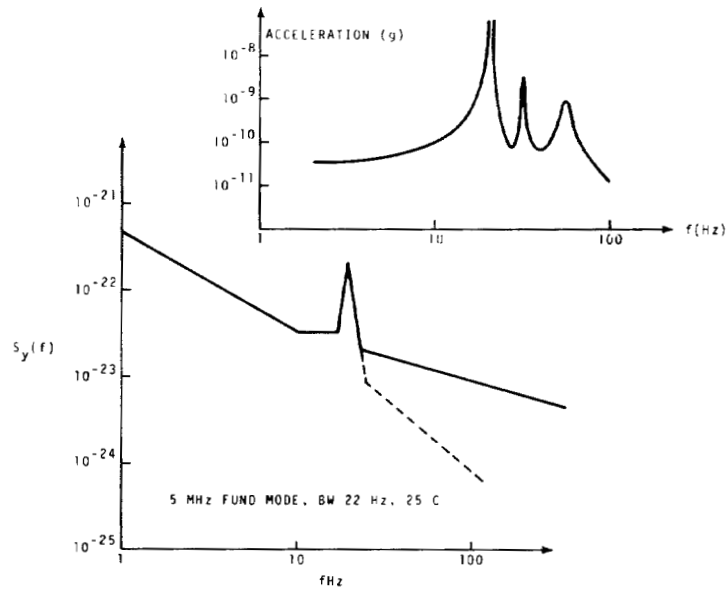


Fig. 5a Density power spectrum correlated with external vibrations

Fig. 5b External vibration amplitude spectrum

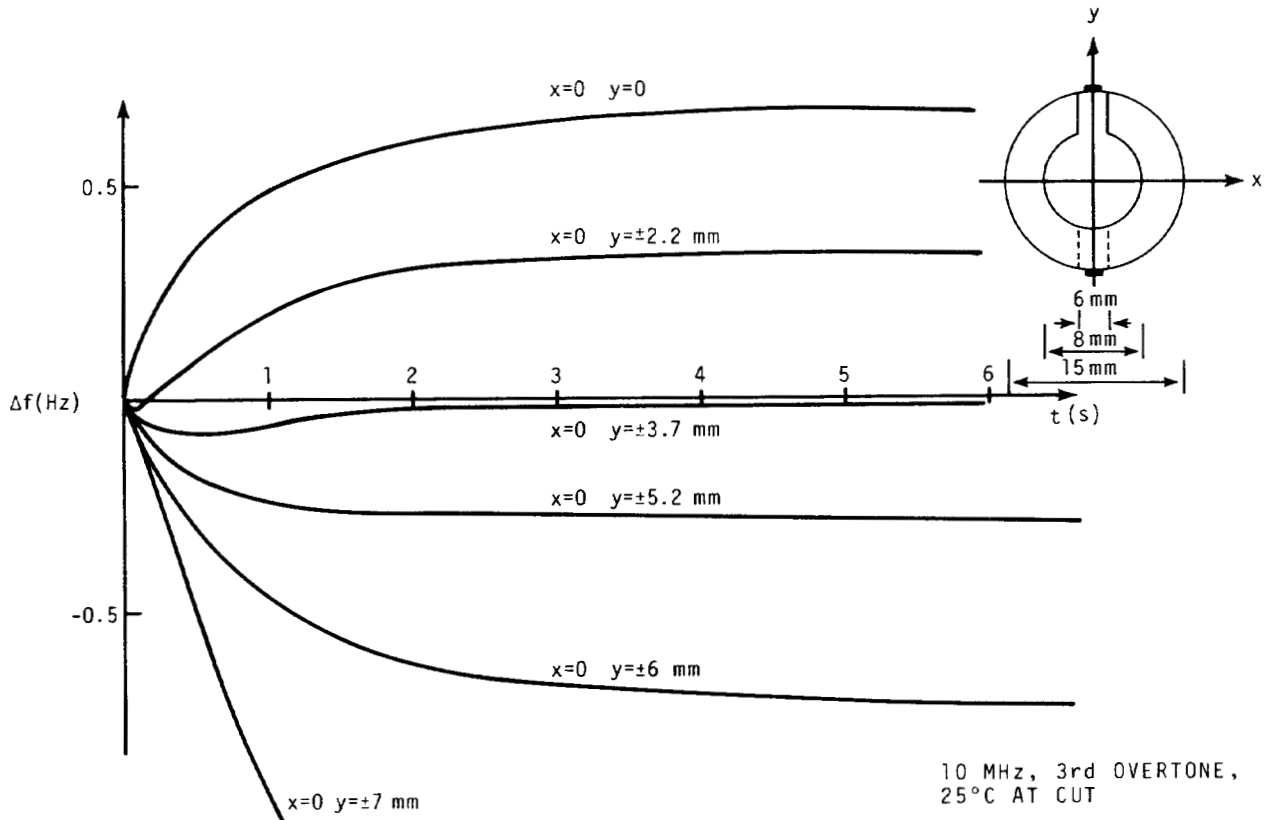


Fig. 6 Frequency response of a resonator: fast temperature variations being applied at different points on the crystal surface.

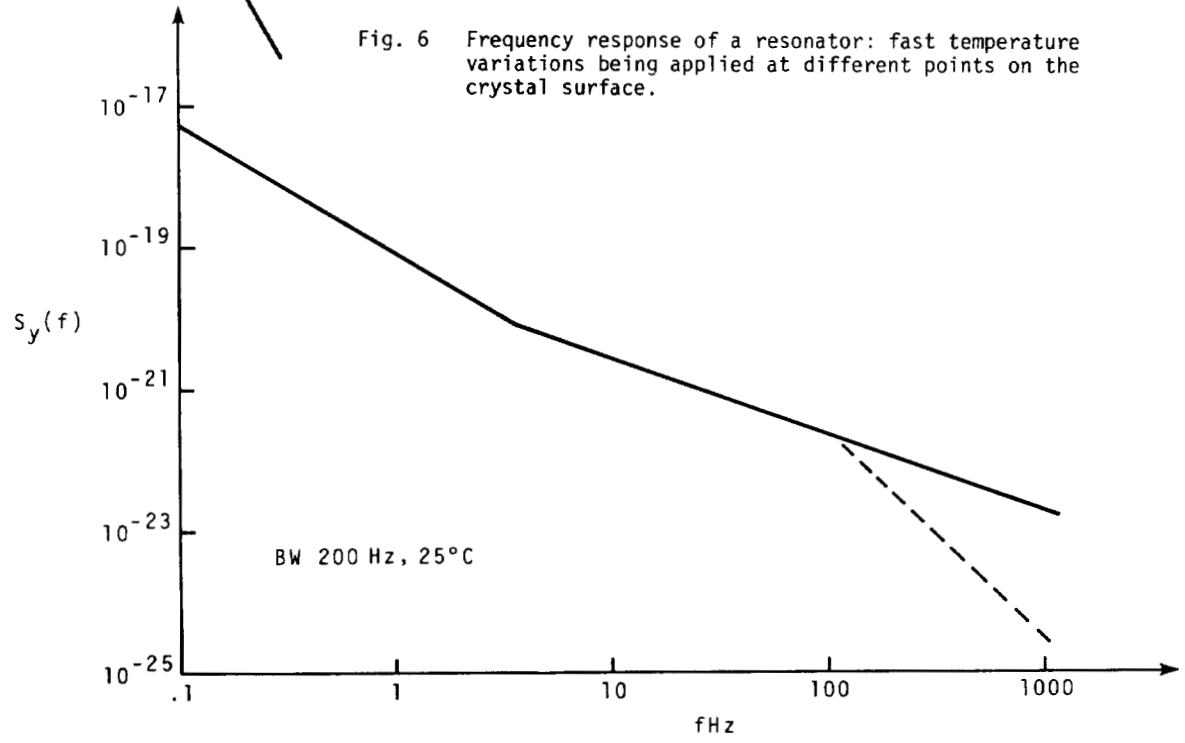


Fig. 7 Fractional frequency fluctuation's density power spectrum of a resonator with a high temperature coefficient (360 Hz/°C)

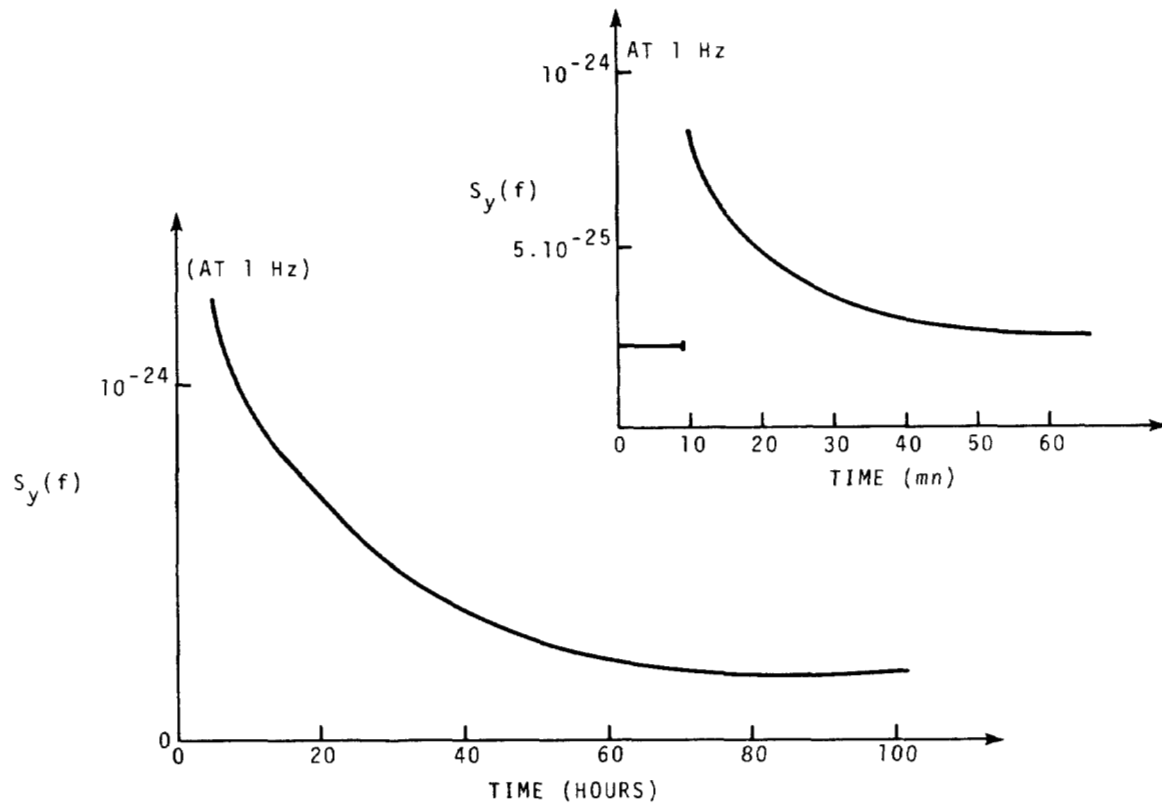


Fig. 8a Density power spectrum at 1 Hz variation versus time, the crystal being oscillating for the first time

Fig. 8b Density power spectrum variations at 1 Hz after a perturbation.